ELSEVIER

www.elsevier.nl/locate/jorganchem

Journal of Organometallic Chemistry 592 (1999) 52–60

Journal of Organometallic Chemistry

Synthesis and properties of organosilicon polymers containing 9,10-diethynylanthracene units with highly hole-transporting properties

Stefan A. Manhart [a], Akira Adachi [a], Koichi Sakamaki [a], Koichi Okita [a], Joji Ohshita [b], Takahiro Ohno [b], Takeshi Hamaguchi [b], Atsutaka Kunai [b,*], Junji Kido [c]

[a] *Japan Chemical Innovation Institute, 5-3 Kuramae 2-Chome, Taito-Ku, Tokyo 111-0051, Japan*
[b] *Department of Applied Chemistry, Faculty of Engineering, Hiroshima University, Higashi-Hiroshima 739-8527, Japan*
[c] *Graduate School of Engineering, Yamagata University, Yonezawa, Yamagata 992-8510, Japan*

Received 22 June 1999; accepted 9 August 1999

Abstract

Coupling reactions of 9,10-di(lithioethynyl)anthracene with dichloromono-, di-, and trisilanes, $Cl(SiR_2)_mCl$ ($m = 1–3$) gave polymers composed of alternating 9,10-diethynylanthracene and organosilicon units. With dichlorotetraorganodisilanes, the corresponding dianthracenophanes composed of two 9,10-diethynylanthracene units linked by tetraorganodisilanylene bridges were also obtained, together with the polymers. The emission spectra of the polymers with di- and trisilanylene units suggest that intrachain aggregation takes place in solution, although it is not obvious for the silanylene polymer. Cyclic voltammetric (CV) analysis of the polymers shows the evident dependence of the CV profiles on the lengths of the silicon chain between the diethynylanthracene units. When the polymer films were treated with $FeCl_3$ vapor, the films became conducting with the maximum conductivities in the order of 10^{-5} S cm^{-1}. The double-layer-type electroluminescent (EL) devices were fabricated using these polymers as a hole-transporting layer and tris(8-quinolinolato)aluminum (III) complex (Alq) as an electron-transporting-emitter layer. The turn-on voltage of the devices became higher and the maximum current density smaller, as increasing the number of silicon atoms in a polymer unit from $m = 1$ to 3. The highest luminance of 1300 cd m^{-2} was obtained from the device based on the silanylene-diethynylanthracene polymer.

Keywords: Organosilicon polymer; Hole transport; Electroluminance

1. Introduction

Polymers with a regular alternating arrangement of an organosilicon unit $–(SiR_2)_m–$ and an aromatic π-electron system (Ar) are currently receiving attention. Enhanced through-space interaction between the π-electron systems by the silicon bridge [1] and/or delocalization of π-electrons through the organosilicon units by σ–π conjugation in the backbone [2] would originate the unique optical and electric properties of these polymers, including red-shifted UV absorptions and semiconducting properties in their doped states [2,3].

Our recent studies on the σ–π conjugated polymers pointed out that extension of the aromatic system significantly influences the properties of the resulting polymers. The photoactivities of disilanylene-polymers $[–Ar_x–(SiR_2)_2–]_n$ (Ar = phenylene [4] and thienylene [5]) decrease with increasing the number of Ar groups (x) in a repeating unit, and the conductivities of the chemically [5] or electrochemically [6] doped thienylene-polymer films tend to increase along increasing x. It has been also demonstrated that the number of silicon atoms (m) in the organosilicon unit influences the properties of the polymers $[–Ar–(SiR_2)_m–]_n$, and the increase of m leads to changes in electronic and optical properties of the polymers arising from the changes of HOMOs and LUMOs from π-type to σ-type [7].

* Corresponding author. Fax: +81-824-227191.

0022-328X/99/$ - see front matter
PII: S0022-328X(99)00481-7

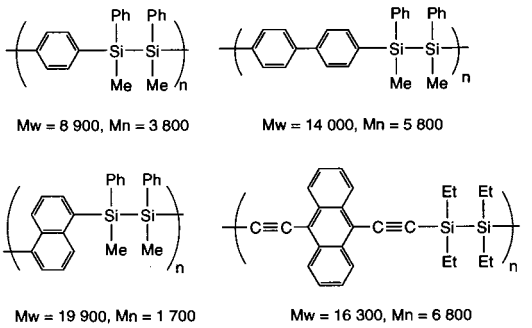

(Chart 1)

Very recently, we have examined a series of polymers shown in Chart 1 regarding their use as the hole-transporting materials in double-layer electroluminescent (EL) devices and found that the turn-on voltages of the devices become lower along the expansion of the π-electron system (Ar) in the order of phenylene < biphenylene < naphthylene < 9,10-diethynylanthracene [8]. The EL device using the diethynylanthracene-polymer shows the best electrical properties and the highest external quantum efficiency of 0.21% among the polymers examined.

In an effort to obtain information for designing polymers with higher hole-transporting properties, we synthesized a series of alternating polymers with mono-, di-, and trisilanylene units $-(SiR_2)_m-$ ($m = 1-3$) and 9,10-diethynylanthracene groups and studied how the length of the organosilicon bridge influences on the EL properties of the polymers. In this paper, we describe the optical, electrochemical, conducting, and hole-transporting properties of the polymers.

2. Results and discussion

2.1. Preparation of polymers with 9,10-diethynylanthracene units

9,10-Diethynylanthracene was readily lithiated by treating with two equivalents of MeLi in ether producing 9,10-di(lithioethynyl)anthracene, which was then treated with dichlorodiethylsilane to give poly[(diethylsilanylene)-9,10-diethynylanthracene] (**1a**) in 66% yield (Scheme 1). Similar reactions of the dilithium reagent with dichloromono-, di-, and trisilanes, $Cl(SiR_2)_mCl$ ($m = 1-3$) gave the corresponding polymers (**1b**, **2a**, **b**, and **3**).

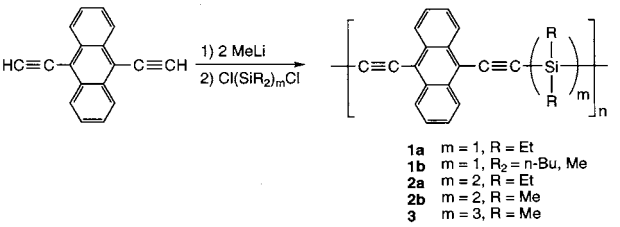

Scheme 1.

Yields, molecular weights, melting points, and glass-transition temperatures of the polymers are summarized in Table 1. Rather low yields of some polymers are ascribed to the formation of oligomers with low molecular weights. Polymers **1a** and **2a**, **b** were readily separated from the oligomers by Soxhlet-extraction with hexane in the pure form as the hexane-insoluble residue. In case of polymer **2a**, only a fraction with high molecular weight is not dissolved in hexane, therefore the isolated yield of the polymer is low. Polymers **1b** and **3** are highly soluble in hexane and purified by reprecipitation from chloroform–isopropyl alcohol.

From the reactions with dichlorodisilanes, anthracenophanes (**4a**, **b** in Chart 2) were isolated from the Soxhlet-extracts. The polymers and anthracenophanes were well characterized by spectroscopic analysis. By the chemical shifts of the dd-signals of the aromatic protons in the ^{1}H-NMR spectra, anthracenophanes **4a**, **b** and polymers **2a**, **b** are readily identified from each others. Thus, the signals for **2a**, **b** appear in the normal range for anthracene ring protons, while for **4a**, **b**, shielding effect of another anthracene unit causes high-field shifts by about 0.5 ppm for the ring protons (see Section 4).

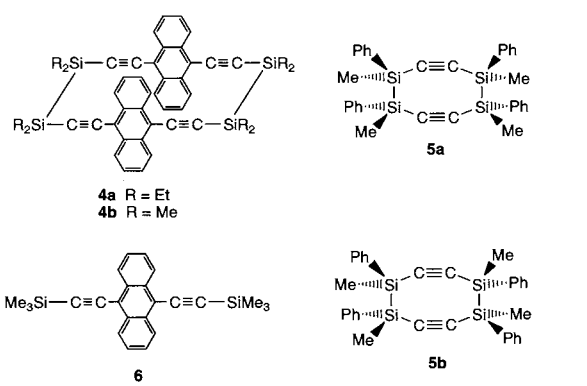

(Chart 2)

Table 1
Synthesis of diethynylanthracene-polymers

Polymer	Yield (%)	M_w (M_n) [a]	NP [b]	m.p. (°C) [c]	T_g (°C) [c]
1a	66	3200 (2100)	6.7	53	15
1b	70	6400 (2900)	8.9	74	– [d]
2a	5	16 300 (6800)	17.2	61	11
2b	38	3700 (2000)	5.9	65	53
3	13	8200 (3800)	9.5	69	−49

[a] Determined by GPC, relative to polystyrene standards.
[b] Number of polymerization = $M_n/(F_w$ of a polymer unit).
[c] Determined by DSC.
[d] Not clear.

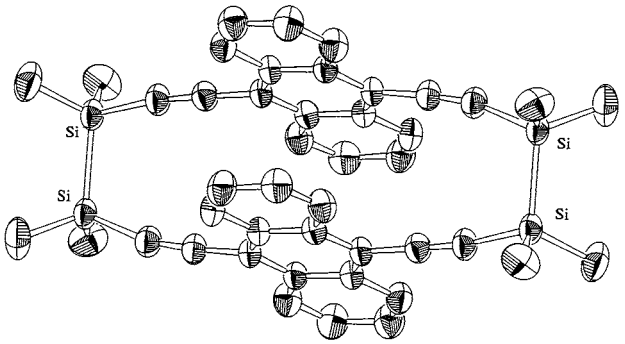

Fig. 1. ORTEP drawing of compound **4b**.

Table 2
Selected bond lengths (Å) and angles (°) for compounds **4b** and **5a**, **b**

	4b	**5a** [a]	**5b** [a]
Bond lengths			
Si–Si	2.358(3)	2.38	2.368
Si–C (sp)	1.839(7), 1.829(7)	1.842	1.831
C≡C	1.192(9), 1.194(9)	1.201	1.2069
Bond angles			
Si–Si–C (sp)	105.7(2), 106.2(2)	103.7	102.8
Si–C≡C	169.1(6), 166.8(7)	166.7	164.3

[a] Values given are averages.

Table 3
UV and CV data for diethynylanthracene-polymers

Polymer	Absorption λ_{max} (nm ($\varepsilon \times 10^{-2}$)) [a]	Oxidation peak potential (V vs. Ag/Ag^+) [b]
1a	448 (295), 419 (208), 394 (91), 271 (495)	(0.80), 1.02, 1.28
1b	447 (262), 418 (195), 394 (91), 272 (703)	(0.80), 1.03, (1.20)
2a	451 (316), 422 (238), 398 (111), 272 (697)	0.80, (0.94), 1.03, (1.24)
2b	449 (272), 421 (223), 406 (437), 263 (843)	(0.64), 0.78, 1.01
3	449 (315), 422 (255), 398 (121), 272 (752)	0.68, (0.90), 1.06

[a] In THF.
[b] On polymer films. Numbers in parentheses indicate potentials for shoulders.

It has been demonstrated that ring-opening polymerization (ROP) of strained organosilacycles under anionic [9], cationic [10], and thermally induced conditions [11] offers a convenient route to the polymers with alternating organosilicon and conjugated units. Attempted ROP of **4a**, **b** in a sealed glass tube with a catalytic amount of methyllithium or tetrabutylammonium fluoride in THF was, however, unsuccessful. With a catalytic amount of $AlCl_3$, WCl_6 or $Pd(PPh_3)_4$, again no reaction occurred. In these experiments, only the starting anthracenophanes were isolated from the reaction mixtures. Thermal treatment of **4a**, **b** by melting at 300°C under an argon atmosphere gave black insoluble materials.

In order to estimate the ring strain in the anthracenophane rings, we determined the crystal structure of **4b** by X-ray diffraction analysis, whose ORTEP drawing is depicted in Fig. 1. Table 2 summarizes selected bond lengths and angles of **4b**, in comparison with those of *cis*,*trans*- and all,*trans*-1,2,5,6-tetramethyl-1,2,5,6-tetraphenyl-1,2,5,6-tetrasilacyclooctadiyne (**5a** and **5b** in Chart 2), which readily undergo anionic and thermally induced ROP to give poly[(1,2-dimethyl-1,2-diphenyldisilanylene)ethynylenes] [9a, 11a]. As can be seen in Table 2, although the bond lengths and angles for the ring of **4b** deviate from their ideal values, the degree of deviation is smaller relative to **5a**, **b**.

Corriu et al. have previously reported the synthesis of poly[(diphenylsilanylene)-9,10-diethynylanthracene] by the Sonogashira-coupling [12] of diethynyldiphenylsilane with 9,10-dibromoanthracene [13]. When we carried out a similar $PdCl_2(PPh_3)_2$-catalyzed reaction of 1,2-diethynyl-1,2-dimethyldiphenyldisilane with 9,10-dibromoanthracene in refluxing triethylamine, a polymer with a low molecular weight of $M_w = 1700$ was obtained. Carrying out the polymerization in a mixed solvent of 1:1 triethylamine–toluene at a reflux temperature led to the formation of the polymer with higher molecular weight ($M_w = 14\,000$). Although ^{1}H-NMR spectra of the polymer samples from the two runs reveal the signals with sufficient integration ratios, the signals are broad and their IR spectra show an Si–O stretching band around 1050 cm^{-1}. These results clearly indicate that cleavage of Si–Si bonds was involved in this polymerization to some extent.

2.2. Optical, electrochemical, and conducting properties of the polymers

Table 3 summarizes the UV absorption maxima of the present diethynylanthracene polymers. They exhibited almost identical UV spectra, independent of the length of the silicon chain and the nature of the substituents on the silicon atoms. The shape of the UV spectra of the polymers is also quite similar to the UV spectrum of a model compound, 9,10-bis(trimethylsilylethynyl)-anthracene (**6** in Chart 2, λ_{max} (ε) = 439 (45 750), 413 (33 220), 390 (14 040), 270 (149 140)). The absorptions in the low-energy region of the polymers are slightly red-shifted by about 10 nm relative to those of model compound **6**. However, the degree of the red-shifts is smaller than that observed for the other alternating polymers composed of alternating organosilicon units and smaller π-electron systems, such as phenylene, ethynylene, and ethenylene, from the respective monomeric compounds [2]. These results clearly indicate that the diethynylanthracene unit is electronically rather isolated and no significant orbital interaction takes place

between the diethynylanthracene π-orbitals and silicon σ-orbitals. This agrees with the results of experimental and theoretical investigations for this type of the polymers, which indicate that the σ–π conjugation is not significantly operative for the polymers with highly extended π-electron systems [2,4,14].

Similar to the UV spectra, the shape of fluorescence spectra of the diethynylanthracene polymers in THF closely resemble that of model compound **6** (λ_{em} (relative intensity) = 420 (31), 437 (100), 469 (51), 500 (12) nm). The polymers exhibit two emission maxima at almost the same wavelengths, around 450 and 480 nm, and a shoulder at about 520 nm regardless of the structure of the silicon chain (Fig. 2). However, an additional shoulder appears at about 560 nm for di- and trisilanylene-polymers **2a** and **3**, probably due to the formation of aggregates. Since the concentrations of the polymers for the fluorescence measurements are sufficiently low (1.9–2.2 mg l^{-1}), interchain aggregation does not seem to play an important role and the shoulders in low energy region are probably due to the intrachain aggregation of diethynylanthracene units. It is likely that the longer silicon chain leads to the higher flexibility of the polymer chain, favoring the intrachain interaction in the solution phase. Similar intrachain aggregation of silylene–divinylbenzene copolymers, whose fluorescence spectra in a solution reveal red-shifted emission bands, has been recently reported [1a].

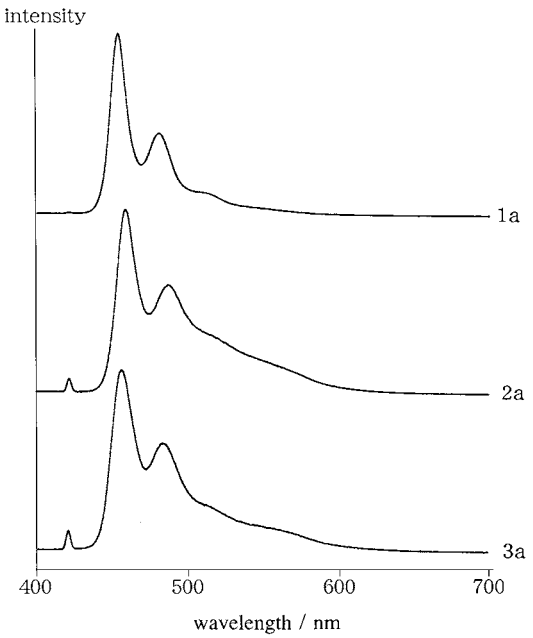

Fig. 2. Fluorescence spectra of **1a**, **2a**, and **3** in THF.

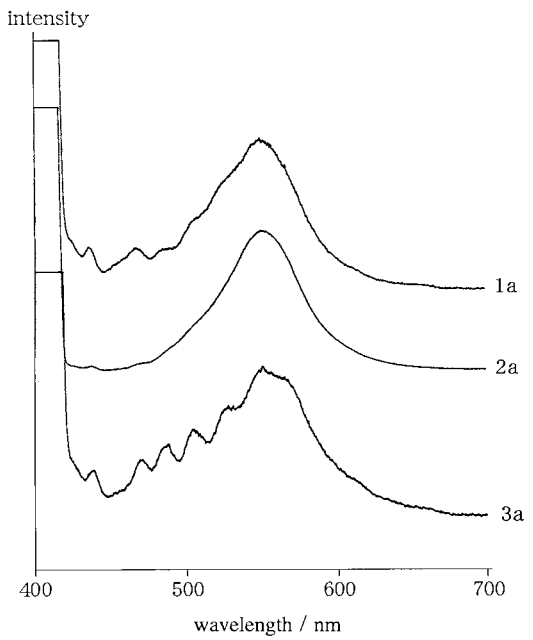

Fig. 3. Fluorescence spectra of **1a**, **2a**, and **3** in the solid state. Small peaks in the range 430–530 nm are ascribed to background emissions.

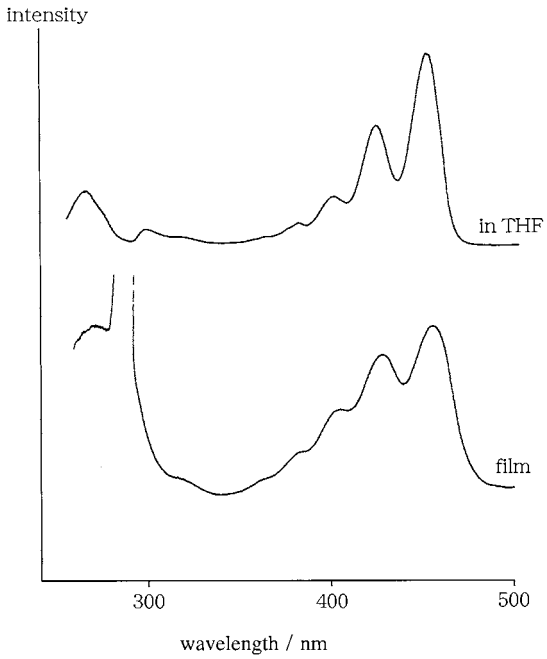

Fig. 4. Excitation spectra of polymer **2a** in THF and in the solid state.

Interestingly, the present polymers exhibit only emission bands at about 560 nm in the solid state (Fig. 3), while the excitation spectra of the polymers in the solid state are identical with those in THF, as illustrated in Fig. 4. Moreover, no obvious dependence of the silicon chain length on the emission profiles is observed in the fluorescence spectra of the polymer films. These results indicate the intensive formation of eximers presumably due to the inter- and/or intrachain aggregation of the diethynylanthracene units, resulting in the red-shifted emission band in the solid state.

Fig. 5 displays cyclic voltammetric profiles for the polymer films, and the anodic peak potentials are sum-

marized in Table 3. As shown in Fig. 5, these polymer films underwent irreversible anodic oxidation in multisteps. In contrast to UV and emission spectra of the polymers, evident influence of the chain length of organosilicon units in the polymer backbone can be seen. The first oxidation potentials move to lower potentials with increasing number of silicon atoms in a unit. One might consider the possibility that the polymer conformations in the solid state affect the CV profiles, e.g. the elongation of silicon chain provides the polymer flexibility in the solid states to facilitate the counter anions to enter into the polymer films. However, such changes in morphology does not seem to be a major reason of the potential shift for the present polymers, since there can be seen no direct correlation between the peak potentials and T_g values (Table 1). The participation of Si–Si bonds is, therefore, inferred as the reason why the first oxidation peak potentials depend on the organosilicon chain length in the present case. Actually, we have recently reported similar electrochemical behaviors of organosilanylene–biphenylylene

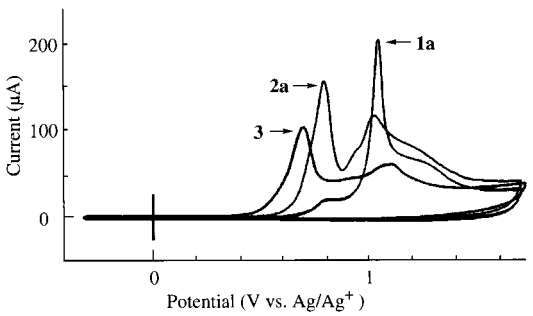

Fig. 5. CV profiles for polymers **1a**, **2a**, and **3**.

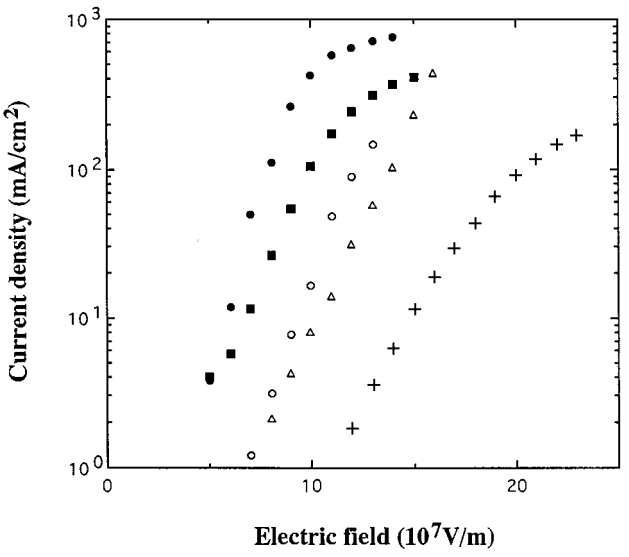

Fig. 6. Current density–voltage curves for EL devices having polymers (●) **1a**; (■) **1b**; (○) **2a**; and (+) **3**, and (△) PVK as the hole-transporting material.

alternating polymers in the solid state [15]. Thus, films of disilanylene–biphenylylene polymers, $[(SiR_2SiR_2)$-4,4′-$(C_6H_4)_2]_n$ (**7**, $R_2 = Me_2$, Et_2, and Ph, Me), undergo irreversible anodic oxidation in two steps at 1.25 V and 1.57 V versus Ag/Ag^+, while films of monosilanylene–biphenylylene, $[(SiMe_2)$-4,4′-$(C_6H_4)_2]_n$ (**8**), and disiloxanylene–biphenylylene polymers $[(SiEt_2OSiEt_2)$–4,4′-$(C_6H_4)_2]_n$ (**9**), reveal a single oxidation peak at 1.65 and 1.49 V, respectively. On the other hand, polymers **7** exhibit UV absorption maxima at 282–283 nm, which are red-shifted only by 7–18 nm from those of **8** and **9**. These are indicative that the Si–Si σ-orbital plays an important role in the first electrochemical oxidation step of the disilanylene–biphenylylene polymers but does not significantly affect the electronic states of these polymers, similar to the present organosilanylene–diethynylanthracene polymers.

The present diethynylanthracene polymers are insulators, but became semiconducting when the thin solid films of the polymers were exposed to $FeCl_3$ vapor under the reduced pressure. The conductivities increased with increasing doping period and reached maximum values in the order of 10^{-5} S cm^{-1} after 20 h of doping. No obvious influence of the structure of the silicon chain on the conducting properties of the polymers was observed. This is in contrast to the fact that the CV profiles of the polymer films are significantly affected by the length of the silicon chain, as described above. The maximum conductivities of the polymers are slightly lower than those reported for poly[disilanylene-1,4-diethynylbenzenes] doped with iodine ($0.56–1.2 \times 10^{-4}$ S cm^{-1}) [16] and comparable to those for $FeCl_3$-doped poly[disilanylenediethynylpyridynes] ($1–3 \times 10^{-5}$ S cm^{-1}) [17].

2.3. Electroluminescent properties of the polymers

Next, we examined hole-transporting properties of the present polymers in a double-layer electroluminescent (EL) system. We constructed three devices with layers of ITO/polymer film/Alq/Mg–Ag in which Alq (tris(8-quinolinolato) aluminum (III)) is used as the electron-transporting-emitting layer and ITO (indium–tin-oxide) and Mg–Ag are the anode and cathode, respectively. We also examined a device having a poly(*N*-vinylcarbazole) (PVK) film as the typical hole-transporting layer instead of diethynylanthracene polymers, for comparison. Fig. 6 shows the current density–electric field curves of these device with different diethynylanthracene polymers. Of these, the devices with silanylene polymers **1a**, **b** exhibited the smallest turn-on electric field (ca. 4×10^7 V m^{-1}), whereas the device with **1a** exhibited higher current density than the device with **1b** at any electric fields applied (up to 1.4×10^8 V m^{-1}) and reached a maximum value of

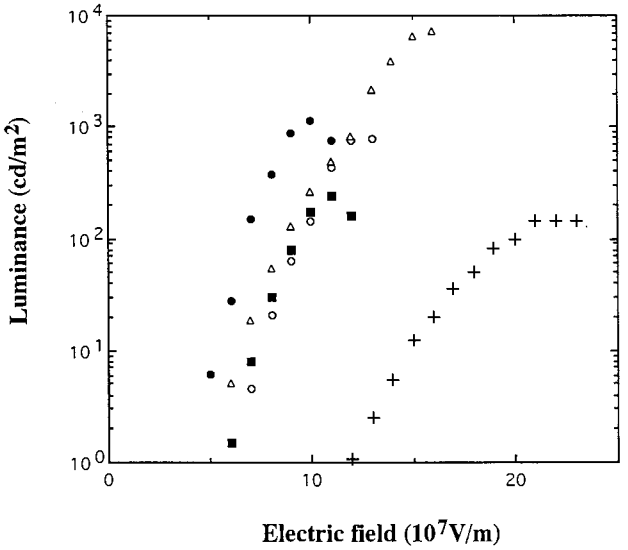

Fig. 7. Luminescence–voltage curves for EL devices having polymers (●) **1a**; (■) **1b**; (○) **2a**; and (+) **3**, and (△) PVK as the hole-transporting material.

760 mA cm^{-2}. As we reported in a previous paper [8], the electrical properties of the device with disilanylene polymer **2a** were almost the same as that with PVK. In contrast, the device with trisilanylene polymer **3** exhibits even higher turn-on electric field and smaller current density at the same operating electric field. These results indicate that hole-transporting properties of the diethynylanthracene polymers are improved in the order of **3** < **2a** < **1b** < **1a** by reducing the number of silicon atoms from the oligosilanylene units. It is most likely that high concentration of diethynylanthracene units in the polymer layer favors the π–π interaction between diethynylanthracene units in an intermolecular way, which plays an important role for improved hole-transporting properties. No evident correlation between the molecular weights or number of polymerization (Table 1) and the current density-electric field profiles are observed.

By applying electric field, each device exhibited green EL whose spectrum was almost identical with the photoluminescence spectrum of vacuum deposited Alq, implying that the EL originated from the Alq layer. As shown in Fig. 7, the device with polymer **1a** emits the light at lower electric field than the other, reaching the highest luminance of 1300 cd m^{-2} at ca. 10×10^7 J m^{-1}. On the other hand, the capability of the device with polymer **3** was found to be the worst among the devices tested, in accord with the current density–electric field characteristics.

3. Conclusions

The silicon chain length in the present diethynylanthracene–organosilicon alternating polymers affects the optical and electrochemical properties of the polymers. A longer silicon chain length provides a higher flexibility in the polymer chain to favor the intrachain aggregation in solution. In the solid state, strong aggregation takes place in inter- and/or intramolecular fashion. Oxidation potentials of the polymer films are also influenced by the silicon chain length and shift to lower potentials with the elongation of the chain.

The silicon chain length has little effect on the conducting properties of the polymer films doped with $FeCl_3$ vapor, but exert significant influence on the hole-transporting properties of the polymers, which are improved by reducing the silicon chain length.

4. Experimental

4.1. General

All reactions were carried out under a dry nitrogen atmosphere. Solvents were purified by distillation from appropriate drying agents under argon. ^{1}H-, ^{13}C- and ^{29}Si-NMR spectra were recorded on Jeol model JNM-EX 270 and JNM-EX 400 spectrometers. UV spectra were measured with a Hitachi U-3210 spectrophotometer. IR-spectra were measured on a Perkin–Elmer 1600-FT infrared spectrometer. Molecular weights of polymers were determined with two Shodex columns, using THF as the eluent, and are relative to polystyrene standards. The actual thickness of each layer on the EL devices was measured with a Sloan Dektak 3030 surface profiler. The emitting area was 0.5×0.5 cm^2. Luminance was measured with a Topcon luminance meter BM-7 at room temperature.

4.2. Materials

9,10-Diethynylanthracene and compound **6** were prepared as reported in the literature [18].

4.3. Preparation of polymers

In a 250 ml three-necked flask was placed 0.67 g (3.0 mmol) of 9,10-diethynylanthracene in 30 ml of ether. To this was added 6.0 ml (6.1 mmol) of a 1.02 M MeLi-diethylether solution at −80°C. The reaction mixture was allowed to warm to room temperature (r.t) and stirred for additional 2 h. After cooling down to −80°C, 0.48 g (3.05 mmol) of dichlorodiethylsilane in 10 ml of ether was added dropwise to the mixture. The reaction mixture was allowed to warm to r.t. and stirred for 12 h. Hydrolysis of the mixture with 50 ml of water, followed by reprecipitation of the organic products from chloroform–ethanol, gave yellow solids. The solids were placed in a Soxhlet apparatus and washed

with ethanol and then with hexane to give 0.61 g (66% yield) of polymer **1** remaining insoluble in hexane: $M_w = 3200$ ($M_w/M_n = 1.5$). IR $\nu_{C\equiv C}$ 2128 cm^{-1}. ^{1}H-NMR ($CDCl_3$): $\delta = 1.14–1.25$, 1.35–1.46 (m, 10H, EtSi), 7.58 (dd, 4H, aromatic H, $J = 6.6$, 3.3 Hz), 8.70 (br. dd, 4H, aromatic H, $J = 6.6$, 3.3 Hz). ^{13}C-NMR ($CDCl_3$): $\delta = 6.9$, 7.8, 103.1, 103.5, 118.5, 121.9, 127.2 (2C), 132.5. Anal. Found: C, 81.82; H, 5.76. $(C_{22}H_{20}Si)_n$. Anal. Calc.: C, 85.11; H, 5.84%. Lower carbon content determined by combustion analysis than the theoretical value is often observed for organosilicon polymers [17,19,20]. This would be due to the formation of carbon-containing ceramics, such as β-SiC during the analysis. In fact, the IR spectrum of the ash obtained from combustion of polymer **1a** at 800°C, the same temperature as used for elemental analysis, shows a strong absorption at 1082 cm^{-1} due to ν_{Si-O} with a weak shoulder around 1200 cm^{-1} due to ν_{Si-C}.

Polymers **1b**, **2a**, **b**, and **3** were prepared as described above. For isolation of anthracenophanes **4a** and **4b**, the Soxhlet-extracts from treatment of **2a**, **b** were evaporated and the residue was recrystallized from hexane. Polymers **1b** and **3** were purified by reprecipitation from chloroform–isopropyl alcohol.

Data for **1b**: yellow solids. $M_w = 6400$ ($M_w/M_n = 2.2$). IR $\nu_{C\equiv C}$ 2130 cm^{-1}. ^{1}H-NMR ($CDCl_3$) 0.78 (3H, s, MeSi), 0.09–1.88 (m, 9H, BuSi), 7.58 (dd, 4H, aromatic H, $J = 6.6$, 3.3 Hz), 8.70 (br. dd, 4H, aromatic H, $J = 6.6$, 3.3 Hz). ^{13}C-NMR ($CDCl_3$) −0.8, 13.9, 16.2, 26.1, 26.3, 103.1, 104.1, 118.4, 127.2 (2C), 132.5. Anal. Found: C, 82.55; H, 6.55. $(C_{27}H_{30}Si)_n$. Anal. Calc.: C, 85.13; H, 6.21%.

Data for **2a**: yellow solids. $M_w = 16\,300$ ($M_w/M_n = 2.4$). IR $\nu_{C\equiv C}$ 2122 cm^{-1}. ^{1}H-NMR ($CDCl_3$) 0.9–1.24 (m, 20H, EtSi), 7.2–7.4 (m, 4H, aromatic H), 8.4–8.65 (m, 4H, aromatic H). ^{13}C-NMR ($CDCl_3$) 5.4, 8.9, 104.1, 105.4, 118.6, 126.7, 127.1, 131.3. ^{29}Si-NMR (δ in $CDCl_3$) −28.2. Anal. Found: C, 78.58; H, 7.21. $(C_{26}H_{28}Si_2)_n$. Anal. Calc.: C, 78.73; H, 7.11%.

Data for **2b**: yellow solids. $M_w = 3700$ ($M_w/M_n = 1.8$). IR $\nu_{C\equiv C}$ 2116 cm^{-1}. ^{1}H-NMR ($CDCl_3$) 0.63 (s, 12H, MeSi), 7.3–7.4 (m, 4H, aromatic H), 8.5–8.6 (m, 4H, aromatic H). ^{13}C-NMR (δ in $CDCl_3$) −2.2, 126.6, 126.8, 127.1, 131.8, signals for acetylene and anthracene *ipso* carbons could not be found due to the low solubility of the polymer in $CDCl_3$. Anal. Found: C, 74.80; H, 5.85. $(C_{22}H_{20}Si_2)_n$. Anal. Calc.: C, 77.59; H, 5.92%.

Data for **3**: yellow solids. $M_w = 8200$ ($M_w/M_n = 2.2$). IR $\nu_{C\equiv C}$ 2124 cm^{-1}. ^{1}H-NMR ($CDCl_3$) 0.47 (s, 6H, MeSi), 0.54 (s, 12H, MeSi), 7.4 (dd, 4H, ring protons, $J = 6.6$, 3.3 Hz), 8.4 (dd, 4H, ring protons, $J = 6.6$, 3.3 Hz). ^{13}C-NMR ($CDCl_3$) −6.6, −1.7, 104.3, 107.1, 118.4, 126.6, 127.1, 132.0. Anal. Found: C, 66.78; H, 6.66. $(C_{24}H_{26}Si_3)_n$. Anal. Calc.: C, 72.36; H, 6.57%.

Data for **4a**: m.p. 290°C. MS m/z 792 [M^+]. IR $\nu_{C\equiv C}$ 2118 cm^{-1}. ^{1}H-NMR (δ in $CDCl_3$) 1.09 (q, 16H, EtSi, $J = 7.9$), 1.36 (t, 24H, EtSi, $J = 7.9$), 6.98 (dd, 8H, aromatic H, $J = 6.6$, 3.3 Hz), 8.01 (dd, 8H, aromatic H, $J = 6.6$, 3.3 Hz). ^{13}C-NMR ($CDCl_3$) 5.1, 9.0, 105.1, 107.7, 117.8, 125.4, 126.6, 130.9. ^{29}Si-NMR (δ in $CDCl_3$) −23.61. UV λ_{max} (THF) 454 (ε 29 700), 420 (50 400), 406 (43 700), 263 (84 300), 222 (37 500). Anal. Found: C, 77.94; H, 7.13. $C_{52}H_{56}Si_4$. Anal. Calc.: C, 78.73; H, 7.11%.

Data for **4b**: m.p. 287°C. MS m/z 680 [M^+]. IR $\nu_{C\equiv C}$ 2121 cm^{-1}. ^{1}H-NMR ($CDCl_3$) 0.61 (s, 24H, MeSi), 6.99 (dd, 8H, aromatic H, $J = 6.6$, 3.3 Hz), 8.01 (dd, 8H, aromatic H, $J = 6.6$, 3.3 Hz). ^{13}C-NMR ($CDCl_3$) −2.6, 106.5, 106.5, 117.7, 125.5, 126.4, 130.8. ^{29}Si-NMR ($CDCl_3$) −33.7. UV λ_{max} (THF) 454 (29 600), 418 (51 400), 261 (74 000), 222 (32 200). Anal. Found: C, 77.09; H, 5.89. $C_{44}H_{40}Si_4$. Anal. Calc.: C, 77.59; H, 5.92%.

4.4. X-ray crystallographic analysis of **4b**

All unique diffraction maxima with $0 < 2\theta < 126.1°$ for **4b** were recorded on a Rigaku AFC-6S automated four-circle diffractometer using graphite-monochromated Cu–K_α radiation ($\lambda = 1.5418$ Å). Refractions with $I > 3\sigma(I)$ were used in the least-squares refinement. The structure was solved by SIR92 direct method [21] and expanded using DIRDIF94 Fourier techniques [22].

Table 4
Crystal data, experimental conditions, and summary of structural refinement for **4b**

Compound	**4b**
Molecular formula	$C_{44}H_{40}Si_4$
Molecular weight	681.14
Space group	$P\bar{1}$
Cell dimensions	
a (Å)	10.492 (2)
b (Å)	12.700 (2)
c (Å)	7.626 (1)
α (°)	106.35 (1)
β (°)	102.72 (1)
γ (°)	80.72 (1)
V (Å^3)	945.7 (3)
Z	1
$D_{calc.}$ (Mg m^{-3})	1.196
$F(000)$	720.00
Crystal size (mm^3)	$0.4 \times 0.3 \times 0.2$
Crystal color	Yellow
(μ) mm^{-1}	3.355
Diffractometer	Rigaku AFC-6S
Temperature (K)	298
Wavelength (Å)	1.5418 (Cu–K_α)
Monochrometer	Graphite crystal
Scan type	$\omega-2\theta$
Scan speed (deg min^{-1})	4
Scan width (°)	$0<2\theta<126.1$
No. of unique reflections	2856
No. of observed reflections ($I>3\sigma(I)$)	2444
R	0.075
R_w [a]	0.100

[a] Weighting scheme is $(\sigma(F_o)^2+0.0004|F_o|^2)^{-1}$.

The non-hydrogen atoms were refined anisotropically. Neutral atom scattering factors were taken from Cromer and Waber [23]. Anomalous dispersion effects were included in $F_{calc.}$ [24]; the values for $\Delta f'$ and $\Delta f''$ were those of Creagh and McAuley [25]. The values for the mass attenuation coefficients are those of Creagh and Hubbel [26]. All calculations were performed using the teXsan [27] crystallographic software package of Molecular Structure Corporation. Cell dimensions, data collections and refinement parameters are listed in Table 4.

4.5. CV measurements for the polymer films

CVs were measured using a three-electrode system in an acetonitrile solution containing 100 mM of tetraethylammonium tetrafluoroborate as the supporting electrolyte. Thin solid films of the polymers were prepared by spin coating of the polymer solution in chloroform on ITO working electrodes. An Ag/Ag^+ electrode and a Pt plate were used as the reference and counter electrode, respectively. Peak potential was determined in a sweep rate of 50 mV s^{-1}. The current–voltage curve was recorded on a Hokuto Denko HAB-151 potentiostat/galvanostat.

4.6. Measurements of conductivities of polymer films doped with $FeCl_3$

Solid films of polymers prepared by spin-coating of polymer chloroform solutions on glass plates were held over ferric chloride powder, which was placed in a glass vessel. Doping was performed under reduced pressure (1 mmHg) by heating the bottom of the glass vessel at 150°C for 24 h. The conductivities of the polymers in vacuo were determined by the four-probe method.

4.7. Preparation of EL devices

A thin film (30–40 nm) of the diethynylanthracene–oligosilanylene polymer was prepared by spin-coating from a solution of polymer in dichloroethane on an anode, indium–tin-oxide (ITO) coated on a glass substrate with a sheet resistance of 15 Ω cm^{-1} (Asahi Glass Company). An electron-transporting-emitting layer was then prepared by vacuum deposition of tris(8-quinolinolato) aluminum (III) (Alq) at 1×10^{-5} torr with a thickness of 60–70 nm on the polymer film. Finally a layer of magnesium–silver alloy with an atomic ratio of 10:1 was deposited on the Alq layer surface as the top electrode at 1×10^{-5} torr.

5. Supplementary material

An ORTEP drawing with a full atomic numbering scheme and tables of atomic coordinates, anisotropic thermal parameters, bond lengths and angles, and observed and calculated structure factors for compound **4b** (22 pages). This material is available on request from J.O.

Acknowledgements

We thank Sankyo Kasei Co. Ltd. and Sumitomo Electric Industry for financial support. We also thank Shin-Etsu Chemical Co. Ltd. for the gift of chlororsilanes. S.A.M. and K.S. are indebted to NEDO for the research fellowship.

References

[1] (a) R.-M. Chen, K.-M. Chien, K.-T. Wong, B.-Y. Jin, T.Y. Luh, J. Am. Chem. Soc. 119 (1997) 11321. (b) C.A. van Walree, M.R. Roest, W. Schuddeboom, L.W. Jenneskens, J.W. Verhoeven, J.M. Warman, H. Kooijman, A.L. Spek, J. Am. Chem. Soc. 118 (1996) 8395.
[2] J. Ohshita, A. Kunai, Acta Polym. 49 (1998) 379.
[3] M. Ishikawa, J. Ohshita, in: H.S. Nalwa (Ed.), Organic Conductive Molecules and Polymers, vol. 2, Wiley, New York, 1997 Chapter 30.
[4] J. Ohshita, T. Watanabe, D. Kanaya, H. Ohsaki, M. Ishikawa, H. Ago, K. Tanaka, T. Yamabe, Organometallics 13 (1994) 5002.
[5] A. Kunai, T. Ueda, K. Horata, E. Toyoda, J. Ohshita, M. Ishikawa, K. Tanaka, Organometallics 15 (1996) 2000.
[6] Y. Kunugi, Y. Harima, K. Yamashita, J. Ohshita, A. Kunai, M. Ishikawa, J. Electroanal. Chem. 414 (1996) 135.
[7] (a) M.-C. Fang, A. Watanabe, M. Matsuda, Chem. Lett. (1994) 13. (b) M.-C. Fang, A. Watanabe, M. Matsuda, J. Organomet. Chem. 489 (1995) 15. (c) M.-C. Fang, A. Watanabe, M. Matsuda, Macromolecules 29 (1996) 6807. (d) M.-C. Fang, A. Watanabe, O. Ito, M. Matsuda, Chem. Lett. 417 (1996). (e) M.-C. Fang, A. Watanabe, M. Matsuda, Polymer 37 (1996) 163.
[8] A. Adachi, S.A. Manhart, K. Okita, J. Kido, J. Ohshita, A. Kunai, Synth. Met. 91 (1997) 333.
[9] (a) M. Ishikawa, T. Hatano, Y. Hasegawa, T. Horio, A. Kunai, A. Miyai, T. Ishida, T. Tsukihara, T. Yamanaka, T. Koike, J. Shioya, Organometallics 11 (1992) 1064. (b) E. Toyoda, A. Kunai, M. Ishikawa, Organometallics 14 (1995) 1089.
[10] K. Shiina, J. Organomet. Chem. 310 (1986) C57.
[11] (a) M. Ishikawa, T. Horio, T. Hatano, A. Kunai, Organometallics 12 (1993) 2078. (b) M. Kira, S. Tokura, Organometallics 16 (1997) 1100.
[12] K. Sonogashira, K. Ohga, S. Takahashi, N. Hagihara, J. Organomet. Chem. 188 (1980) 237.
[13] R.J.P. Corriu, W.E. Douglas, Z.-X. Yang, J. Polym. Sci. Part C Polym. Lett. 28 (1990) 431.
[14] K. Tanaka, H. Ago, T. Yamabe, M. Ishikawa, T. Ueda, Organometallics 13 (1994) 5583.
[15] J. Ohshita, K. Sugimoto, A. Kunai, Y. Harima, K. Yamashita, J. Organomet. Chem. 850 (1999) 77.
[16] C.-H. Yuan, R. West, Appl. Organomet. Chem. 8 (1994) 423.
[17] A. Kunai, E. Toyoda, K. Horata, M. Ishikawa, Organometallics 14 (1995) 714.
[18] E. Kobayashi, J. Jiang, H. Ohta, J. Furukawa, J. Polym. Sci. A Polym. Chem. 28 (1990) 2641.

[19] J. Ohshita, M. Ishii, Y. Ueno, A. Yamashita, M. Ishikawa, Macromolecules 27 (1994) 5583.
[20] H.-G. Woo, J.F. Walzer, T.D. Tilley, Macromolecules 24 (1991) 6843.
[21] A. Altomare, M.C. Burla, M. Camalli, M. Cascarano, C. Giacovazzo, A. Guagliardi, G. Polidori, J. Appl. Cryst. (1994).
[22] P.T. Beurskens, G. Admiraal, G. Beurskens, W.P. Bosman, R. de Gelder, R. Israel, J.M.M. Smits, The DIRDIF-94 program system, Technical Report of the Crystallography Laboratory, University of Nijmegen, The Netherlands, 1994.
[23] D.T. Cromer, J.T. Waber, in: International Tables for X-ray Crystallography, vol. IV, Table 2.2A, Kynoch, Birmingham, UK, 1974.
[24] J.A. Ibers, W.C. Hamilton, Acta Crystallogr. 17 (1964) 781.
[25] D.C. Creagh, W.J. McAuley, in: A.J.C. Wilson (ed.), International Tables for Crystallography, vol C, Table 4.2.6.8, Kluwer, Boston, 1992, pp. 219–222.
[26] D.C. Creagh, J.H. Hubbell, in: A.J.C. Wilson (ed.), International Tables for Crystallography, Table 4.2.4.3, Kluwer, Boston, 1992, pp. 200–206.
[27] teXsan, Crystal Structure Analysis Package, Molecular Structure Corporation, 1985 and 1992.